Energy Proceedings
Vol 36, 2023
ISSN 2004-2965

Demand-side management of residential PV-battery-flexible load systems considering the interests of end-users, grid operators, and national governments

Zhengyi Luo[1,2], Jinqing Peng[1,2*]
1 College of Civil Engineering, Hunan University, Changsha, Hunan, China
2 Key Laboratory of Building Safety and Energy Efficiency of the Ministry of Education, Changsha, Hunan, China
(*Corresponding Author: jqpeng@hnu.edu.cn)

ABSTRACT

The proper scheduling of residential demand-side flexible resources, such as static batteries and flexible loads, is crucial for mitigating the impacts of intermittent and fluctuating residential rooftop PV generation on utility grids. Previous studies have often overlooked the benefits of different stakeholders involved in the optimal scheduling process. To address these gaps, this study proposed a comprehensive framework for the many-objective optimal dispatch of residential PV-battery-flexible load systems, considering the interests of users, grid operators, and governments. Specifically, a day-ahead optimal dispatch model with six objective functions relevant to the three stakeholders' benefits was developed. The effectiveness of the framework was validated through case studies, which demonstrated a significant improvement in system performance compared to the maximizing self-consumption strategy. The proposed framework can provide valuable guidance for the optimal scheduling of residential PV-battery-flexible load systems in practice.

Keywords: residential PV-battery-flexible load systems, demand-side management, optimal scheduling, different stakeholders

1. INTRODUCTION

Developing renewable energy generation technology is an important way to achieve the goal of carbon neutrality. The government has introduced a large number of favorable policies to promote the application of photovoltaic (PV) power generation and wind power generation. More and more PV panels are installed on the roofs of residential buildings, transforming buildings from traditional consumers to prosumers. The increasing proportion of PV generation would have a significant impact on the stable operation of utility grids. How to manage the demand-side flexible resources of residential buildings to decrease the influence of intermittent PV generation on the grid is a great challenge.

A common way to manage the demand-side flexible resources of residential buildings is to perform the day-ahead optimal scheduling with some certain optimization objectives to obtain the optimal operation schemes. The energy costs were selected as optimization objectives to conduct the scheduling optimization in numerous studies [1–3]. Moreover, some literature was to maximize occupant's thermal comfort [4,5]. Few studies also focused on the impacts of household electricity consumption on utility grids [6]. However, these studies only focused on one or two optimization objectives. A comprehensive consideration of various optimization objectives is necessary, due to the optimal dispatch involving the benefits of various stakeholders, including end-users, grid operators, and national governments.

2. METHODOLOGY

A typical residential home energy system, called PV-battery-flexible load system, is introduced first. Then, the proposed optimization models to perform the day-ahead optimal scheduling of PV-battery-flexible load systems is described in details.

2.1 A typical residential PV-battery-flexible load system

A typical resident PV-battery-flexible load system is shown in **Fig. 1**. Distributed PV generation and battery banks are configured to satisfy household electricity loads, including flexible loads and inflexible loads. The system is connected with utility grids and can exchange power with the grid. Moreover, the flexible loads include thermostatically controlled loads (TCLs) and deferrable loads, which can be scheduled to provide grid services.

This is a paper for the 9th Applied Energy Symposium: Low Carbon Cities and Urban Energy Systems (CUE2023), Sep. 2-7, 2023, Matsue & Tokyo, Japan.

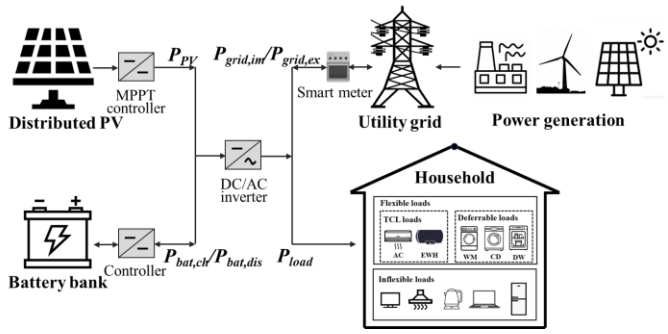

Fig. 1. *A typical residential PV-battery-flexible load system.*

2.2 Optimization models

A many-objective nonlinear optimization model was developed to perform the day-ahead optimal scheduling of PV-battery-flexible load systems. The details of the model, including the optimization variables, objective functions, and constraints are introduced in this section.

2.2.1 Optimization variables

The optimization variables of the model are TCLs' temperature setpoints, deferrable loads' start-up time, and battery's charging/discharging power, as presented in Eq. (1). In this equation, T_{tcl}^{set} is the decision variable regrading TCLs' temperature setpoints; τ_{tcl}^{start} and τ_{tcl}^{end} are the turn-on moment and turn-off moment of TCLs, which depend on occupants. Since the operation of TCLs is featured by 'part-time-part-space' in China, which is not throughout the day, the occupant behaviors of TCLs usage were considered in this study. Moreover, τ_{shift}^{start} is the decision variable on the start-up time of deferrable loads. P_{bat} is the decision variable about the charging/discharging power of battery banks, and *N* is the total amount of timesteps.

$$X = [T_{tcl}^{set}(\tau_{tcl}^{start}), \dots, T_{tcl}^{set}(\tau_{tcl}^{end}), \tau_{shift}^{start}, P_{bat}(1), \dots, P_{bat}(N)] \quad (1)$$

2.2.2 Objective functions

Moreover, six optimization objectives were selected in the developed optimal model considering the benefits of end-users, grid operators, and national governments. The optimization objectives are to minimize household's daily operation costs, user dissatisfaction, the peak-valley difference, CO_2 emissions, and to maximize the self-consumption rate (SCR) and self-sufficiency rate (SSR) of PV generation, as described below.

The daily operation costs were calculated by Eqs. (2)-(6), where Eq. (3), Eq. (4), Eq. (5), and Eq. (6) are to calculate the operation costs of PV, the costs of battery degradation, electricity bills, and the bonus from feeding the distributed PV generation into utility grids, respectively.

$$F_1(X) = min\big(C_{pv} + C_{bat} + C_{grid,im} - C_{grid,ex}\big) \quad (2)$$

$$C_{pv} = P_{pv}^{nom} \cdot \epsilon_{pv} \cdot \Delta\tau \cdot T / L_{cyc}^{pv} \quad (3)$$

$$C_{bat} = \left(\frac{1 - SOH}{1 - \alpha_{rep}}\right) \cdot \epsilon_{bat} \cdot E_{bat}^{nom} \quad (4)$$

$$C_{grid,im} = \sum_{\tau=1}^{T} \epsilon_{g,im}(\tau) \cdot P_{grid,im}(\tau) \cdot \Delta\tau \quad (5)$$

$$C_{grid,ex} = \sum_{\tau=1}^{T} FiT \cdot P_{grid,ex}(\tau) \cdot \Delta\tau \quad (6)$$

where C_{pv}, C_{bat}, $C_{grid,im}$, and $C_{grid,ex}$ are the operation costs of PV, the costs of battery degradation, electricity bills, and the bonus from selling power; P_{pv}^{nom} and E_{bat}^{nom} are the rated capacity of PV arrays and batters; ϵ_{pv} and ϵ_{bat} are the unit capital cost of PV and batteries; $\epsilon_{g,im}$ and *FiT* are the electricity price tariffs and the feed-in-tariff; $P_{grid,im}$ and $P_{grid,ex}$ are the power imported from utility grids and the power fed into utility grids; *T* is the number of timesteps; L_{cyc}^{pv} is the life time of PV arrays.

User's dissatisfaction was expressed by Eqs. (7)-(10), according to Ref. [7]. Eqs. (8)-(10) is to calculate the dissatisfaction φ_{tcl} caused by changing TCLs' temperature setpoints, while Eq. (32) is to calculate the dissatisfaction φ_{shift} from the shifting of deferrable load's start-up time.

$$F_2(X) = min\big(\omega_{tcl}\varphi_{tcl} + \omega_{shift}\varphi_{shift}\big) \quad tcl \in \{ACs, EWHs\}; shift \in \{WMs, clothes\ dryers, dishwashers\} \quad (7)$$

$$\varphi_{tcl} = \frac{\sum_{\tau_{start}}^{\tau_{end}} \frac{e^{\psi_{tcl}(\tau)} - 1}{e - 1}}{N_{tcl}} \quad (8)$$

$$\psi_{tcl}(\tau) = \frac{\left|T_{tcl}^{set}(\tau) - T_{tcl}^{set,pre}\right|}{T_{tcl}^{set,max} - T_{tcl}^{set,min}} \quad (9)$$

$$\varphi_{shift} = \frac{\left|\tau_{shift}^{start} - \tau_{shift}^{start,pre}\right|}{\tau_{shift}^{start,max} - \tau_{shift}^{start,min}} \quad (10)$$

where ω_{tcl} and ω_{shift} are the weights; τ_{start} and τ_{end} are the turn-on moment and turn-off moment of

TCLs; ψ_{tcl} denotes the degree that the optimal TCL's temperature setpoint $T_{tcl}^{set}(\tau)$ deviates from occupants desired setting value $T_{tcl}^{set,pre}$; $T_{tcl}^{set,max}$ and $T_{tcl}^{set,min}$ are the upper and lower limits of occupant preference of TCL's temperature setting; τ_{shift}^{start} is the optimized deferrable load's turn-on moment; $\tau_{shift}^{start,pre}$ is occupants desired turn-on moment, $\tau_{shift}^{start,max}$ and $\tau_{shift}^{start,min}$ are the upper and lower limits of flexibility window.

The peak-valley difference of net power profiles was formulated by Eq. (11), where P_{grid}^{peak} is the peak power of net power profiles and P_{grid}^{valley} is the valley power of net power profiles.

$$F_3(X) = min\left(P_{grid}^{peak} - P_{grid}^{valley}\right) \quad (11)$$

The SCR of PV generation was calculated by Eq. (12), where $E_{pv-load}$ is the PV generation that was consumed by loads, and E_{pv} is the total PV generation.

$$F_4(X) = max\left(\frac{E_{pv-load}}{E_{pv}}\right) \quad (12)$$

The SSR of PV generation was formulated by Eq. (13), where E_{load} is the total loads of household.

$$F_5(X) = max\left(\frac{E_{pv-load}}{E_{load}}\right) \quad (13)$$

The daily CO_2 emissions were expressed by Eq. (14), where ϕ is the CO_2 emission coefficient of the power purchased from utility grids, and $E_{grid-load}$ is the electricity consumed by loads among the power purchased from utility grids.

$$F_6(X) = min\left(\phi \cdot E_{grid-load}\right) \quad (14)$$

2.2.3 Constraints

The constraints of the model include occupant behaviors constraints and energy balance constraints, which are described as follows.

The occupant behaviors constraints include the limits on the optimization variables regarding TCLs' temperature setpoints and deferrable loads' start-up time, as presented by Eq. (15) and Eq. (16). In these equations, [$T_{tcl}^{set,min}$, $T_{tcl}^{set,max}$] is the TCL's temperature setpoint range that occupants are used to setting; [$\tau_{shift}^{start,min}$, $\tau_{shift}^{start,max}$] is the periods that occupants are used to using deferrable household appliances, such as WMs, clothes dryers, and dishwashers. The limits on the optimization variables of battery's charging/discharging power are shown in Eq. (17), where $P_{bat}^{dis,max}$ and $P_{bat}^{ch,max}$ are the maximum discharging power and charging power of the battery. Moreover, occupant behaviors of flexible household appliances use, such as daily use frequency, start time of operation, and operation duration, were used as operation constraints of flexible loads. The parameters relevant to occupant behaviors were determined by statistical analysis based on the historical operation of flexible loads.

$$T_{tcl}^{set,min} \le T_{tcl}^{set}(\tau) \le T_{tcl}^{set,max} \quad (15)$$

$$\tau_{shift}^{start,min} \le \tau_{shift}^{start} \le \tau_{shift}^{start,max} \quad (16)$$

$$P_{bat}^{dis,max} \le P_{bat}(\tau) \le P_{bat}^{ch,max} \quad (17)$$

The energy balance constraints were formulated by Eq. (18). In this equation, $P_{grid}(\tau)$ is the power that households exchanged with utility grids; $P_{pv}(\tau)$ is the power of PV; $P_{bat}(\tau)$ is the power of batteries; $P_{tcl}(\tau)$ is the power of TCLs; $P_{shift}^{in}(\tau)$ is the power of deferrable loads; $P_{inflex}(\tau)$ is the power of household inflexible loads. $P_{pv}(\tau)$, $P_{bat}(\tau)$, $P_{tcl}^{in}(\tau)$, $P_{shift}^{in}(\tau)$, and $P_{inflex}(\tau)$ were calculated by the models of PV, battery banks, TCLs, deferrable loads, and inflexible loads. The details are described as follows.

$$P_{grid}(\tau) = P_{bat}(\tau) + P_{tcl}(\tau) + P_{shift}^{in}(\tau) + P_{inflex}(\tau) - P_{pv}(\tau) \quad (18)$$

The output power of PV was calculated by Eqs. (19)-(21) [8].

$$P_{pv}(\tau) = G_s(\tau) \cdot A_{pv} \cdot \eta_{STC} \cdot \eta_T(\tau) \cdot \eta_{inverter} \quad (19)$$

$$\eta_T(\tau) = 1 + \gamma \cdot (T_{module}(\tau) - T_{STC}) \quad (20)$$

$$T_{module}(\tau) = T_{en}(\tau) + G_s(\tau) \cdot \left(\frac{T_{NOCT} - 20}{800}\right) \quad (21)$$

where P_{pv} is the power of PV generation; G_s is the solar radiation; A_{pv} is the areas of installed PV arrays; η_{STC} is the power generation efficiency of PV arrays under standard test conditions (STC); η_T is the correction factor, representing the power loss deriving from PV module temperature rising; $\eta_{inverter}$ is inverter's conversion efficiency; γ is PV modules' power temperature coefficient; T_{module} is PV modules' operation temperature; T_{STC} is PV modules' temperature under STC; T_{en} is the ambient temperature, ºC; T_{NOCT} is PV modules' Nominal Operating Cell Temperature (NOCT); τ is time slot. The

forecasted meteorological data was obtained from the local Meteorological Administration through an Application Program Interface (API).

For the model of battery banks, it can be expressed by Eq. (22) [9], where SOC is the state of charge of the battery. Eq. (23) is the operation constraints of the battery. Moreover, the degradation of the battery was formulated by Eqs. (24)-(26) [10], which is the results of battery's charging and discharging. The degradation would cause the decreasing of the state of health (SOH) of the battery, which can be calculated by Eq. (27)

$$SOC(\tau) = SOC(\tau-1) + \left[\frac{\pi \cdot P_{bat}(\tau)\cdot \eta_{ch}}{E_{bat}^{nom}} + (1-\pi)\frac{P_{bat}(\tau)}{\eta_{dis}\cdot E_{bat}^{nom}}\right]\cdot \Delta\tau \quad (22)$$

$$SOC_{min} \le SOC(t) \le SOC_{max} \quad (23)$$

$$\beta_{bat}^{tot}(\tau) = \beta_{bat}^{cal}(\tau) + \beta_{bat}^{cyc}(\tau) \quad (24)$$

$$\beta_{bat}^{cal}(\tau) = [6.6148\times 10^{-6}\times SOC(\tau) + 4.6404\times 10^{-6}]\cdot \frac{\Delta\tau}{60} \quad (25)$$

$$\beta_{bat}^{cyc}(\tau) = 0.5 \cdot \frac{\left|\pi\cdot P_{bat}^{ch}(\tau) - (1-\pi)\cdot P_{bat}^{dis}(\tau)\right|\cdot \Delta\tau}{L_{cyc}^{bat}\cdot E_{bat}^{nom}} \quad (26)$$

$$SOH(\tau) = 1 - 0.2\times \beta_{bat}^{tot}(\tau) \quad (27)$$

where P_{bat} is battery's charging/discharging power; η_{ch} is battery's charging efficiency; η_{dis} is battery's discharging efficiency; π is a binary variable; $\Delta\tau$ is time intervals; SOC_{min} is the minimum value of battery's SOC, while SOC_{max} is the maximum value of that; $P_{bat}^{dis,max}$ and $P_{bat}^{ch,max}$ are the maximum discharging power and charging power of the battery; β_{bat}^{tot} is the total degradation of the battery; β_{bat}^{cal} and β_{bat}^{cyc} are the calendric aging and the cyclic aging; L_{cyc}^{bat} is the life time of the battery; E_{bat}^{nom} is the rated capacity of the battery.

TCLs in residential buildings mainly include air conditioners (ACs) and water heaters. The operating power of ACs can be formulated by Eqs. (28)-(32) [11].

$$P_{ac}(\tau) = \begin{cases} 0, & \tau < \tau_{ac}^{start} \text{ or } \tau > \tau_{ac}^{end} \\ P_{ac}^{in}(\tau), & \tau_{ac}^{start} \le \tau \le \tau_{ac}^{end} \end{cases} \quad (28)$$

$$P_{ac}^{in}(\tau) = U_{ac}(\tau)\cdot P_{ac}^{on} + [1-U_{ac}(\tau)]\cdot P_{ac}^{off} \quad (29)$$

$$U_{ac}(\tau) = \begin{cases} 0, & T_a(\tau) < T_{ac}^{set}(\tau) - \frac{\delta_{ac}}{2} \\ 1, & T_a(\tau) > T_{ac}^{set}(\tau) + \frac{\delta_{ac}}{2} \\ U_{ac}(\tau-1), & T_{ac}^{set}(\tau) - \frac{\delta_{ac}}{2} \le T_a(\tau) \le T_{ac}^{set}(\tau) + \frac{\delta_{ac}}{2} \end{cases} \quad (30)$$

$$T_a(\tau+1) = k_1 T_a(\tau) + k_2 T_{en}(\tau) \pm k_3 P_{ac}^{in}(\tau) EIR(\tau) + k_4 G_s(\tau) + k_5 \quad (31)$$

$$EIR(\tau) = [0.0193\cdot T_{en}(\tau) + 0.3259]\cdot EIR_{nom} \quad (32)$$

where P_{ac}^{in} is AC's operating power; τ_{ac}^{start} and τ_{ac}^{end} are the turn-on moment and turn-off moment of ACs; P_{ac}^{on} and P_{ac}^{off} are the AC's operating power in ON and OFF states, respectively; U_{ac} is a binary variable that 1 denotes that ACs operate in ON state and 0 denotes that ACs operate in OFF state; T_a is the indoor air temperature; T_{ac}^{set} is AC's temperature setpoint; δ_{ac} is the thermostat dead-band; k_1, k_2, k_3, k_4, and k_5 are model parameters; T_{en} is the outdoor temperature; G_s is the solar radiation; EIR is AC's energy input ratio and can be calculated by Eq. (32) [12].

Similar to the model of ACs, the model of electric resistance water heaters (EWHs) was expressed by Eqs. (33)-(36).

$$P_{ewh}(\tau)=\begin{cases}0, & \tau<\tau_{ewh}^{start}\ or\ \tau>\ \tau_{ewh}^{end}\\ P_{ewh}^{in}(\tau), & \tau_{ewh}^{start}\le\tau\le\ \tau_{ewh}^{end}\end{cases} \tag{33}$$

$$P_{ewh}^{in}(\tau)=U_{ewh}(\tau)\cdot P_{ewh}^{on} \tag{34}$$

$$U_{ewh}(\tau)=\begin{cases}0,\ T_w(\tau)\ge T_{ewh}^{set}(\tau)\\ 1, T_w(\tau)\le T_{ewh}^{set}(\tau)-\delta_{ewh}\\ U_{ewh}(\tau-1), T_{ewh}^{set}(\tau)-\delta_{ewh}<T_w(\tau)<T_{ewh}^{set}(\tau)\end{cases} \tag{35}$$

$$T_w(\tau+1)=k_1'T_w(\tau)+k_2'T_{am}(\tau)+k_3'P_{ewh}^{in}(\tau)+k_4'P_{use}(\tau)+k_5' \tag{36}$$

where P_{ewh}^{in} is the EWH's operating power; τ_{ewh}^{start} and τ_{ewh}^{end} are the turn-on moment and turn-off moment of EWHs; P_{ewh}^{on} is the EWH's operating power in ON state; U_{ewh} is a binary variable that 1 denotes that EWHs operate in ON state and 0 represents that EWHs operate in OFF state; T_w is the hot water temperature; T_{ewh}^{set} is EWH's temperature setpoint; δ_{ewh} is the thermostat dead-band; k_1', k_2', k_3', k_4', and k_5' are model parameters; T_{am} is the ambient temperature; P_{use} is the heat loss caused by hot water consumptions.

In addition to the TCLs, the model of deferrable loads was formulated by Eqs. (37) and (38), according to their operation characteristics.

$$P_{shift}^{in}(\tau)=\begin{cases}P_{shift}^{i,1},\ \tau\in[\tau_{shift}^{start},\tau_{shift}^{start}+\Delta\tau_{shift}^{i,1}]\\ P_{shift}^{i,2},\ \tau\in[\tau_{shift}^{start}+\Delta\tau_{shift}^{i,1},\tau_{shift}^{start}+\Delta\tau_{shift}^{i,1}+\Delta\tau_{shift}^{i,2}]\\ \cdots\cdots\\ P_{shift}^{i,m},\ \tau\in[\tau_{shift}^{start}+\Delta\tau_{shift}^{i,1}+\cdots+\Delta\tau_{shift}^{i,m-1},\tau_{shift}^{start}+\Delta\tau_{shift}^{i,1}+\cdots+\Delta\tau_{shift}^{i,m}]\\ 0,\ \text{other}\end{cases} \tag{37}$$

$$\Delta\tau_{shift}^{i}=\sum_{m=1}^{M}\Delta\tau_{shift}^{i,m} \tag{38}$$

where P_{shift}^{in} is the operating power of deferrable loads; $P_{shift}^{i,m}$ is deferrable load's operating power at operation stage *m* with operation mode *i*; $\Delta\tau_{shift}^{i,m}$ is the duration of operation stage *m* with operation mode *i*; τ_{shift}^{start} is the time that deferrable loads start to work; $\Delta\tau_{shift}^{i}$ is the total duration of the operation mode *i*.

Additionally, the power profiles of inflexible loads were predicted using the persistence forecast method [13]. This method involves calculating the average daily power profiles of inflexible loads from the past few days, which then serves as the forecasted power profiles of inflexible loads. Additionally, separate datasets were considered for weekdays and weekends, as the power consumption of inflexible loads varies between these two categories.

2.3 Solution methods

After the optimal model was formulated, the reference-point-based Non-dominated Sorting Genetic Algorithm (NSGA-III) [14] was employed to solve the model with the Pareto solution set obtained. The Technique for Order Preference by Similarity to an Ideal Solution (TOPSIS) approach was used to pick out the final solution from the Pareto solution set. The details processes of the solution methods are presented in **Fig. 2**.

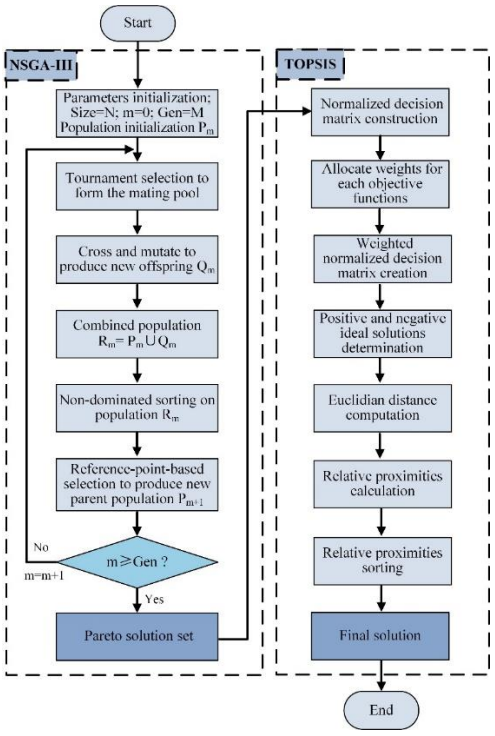

Fig. 2. *Processes of the solution method.*

Table 1. Occupant behaviors of flexible loads.

Flexible loads	$[T_{tcl}^{set,min}, T_{tcl}^{set,max}]$			$[\tau_{shift}^{start,min}, \tau_{shift}^{start,max}]$	
	AC1	AC2	EWH	Washing machines	Dishwashers
Values	[22, 28 ºC]	[24, 29 ºC]	[60, 70 ºC]	[5:00, 8:00]	[19:00, 6:00]

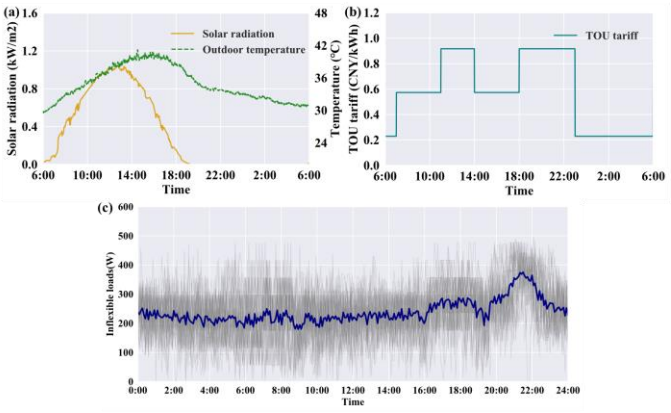

Fig. 3. *(a) Environment data; (b) Electricity tariffs; (c) The monitored electricity profiles of inflexible loads and the average power profiles of inflexible loads.*

3. CASE STUDY

A typical rural family in hot-summer and cold-winter zone of China was chosen in this study. The operation data of the household flexible loads, including two room ACs, an EWH, a washing machine, and a dishwasher, were monitored with the power consumption profiles of the household also measured. The pilot test began in July 2022 and lasted for two months. The monitored data was used to develop the flexible load models and identify occupant behaviors. Based on these identified models, the day-ahead optimal scheduling was performed.

3.1 Input data

Based on the monitored operation data of the flexible loads, occupant behaviors were identified by the statistical analysis methods, as listed in **Table 1**. Furthermore, the ambient parameters and electricity tariffs are presented in **Fig. 3(a)** and **Fig. 3(b),** respectively. The monitored power profiles of inflexible loads and the average power profiles of inflexible loads are illustrated in **Fig. 3(c)**.

3.2 Results and discussion

The demand-side management strategy of the PV-battery-flexible load system was discussed under various operation strategies in this section. Two cases were set with the details described below.

- Case 1: The PV-battery-flexible load system operates under a traditional rule-based operation strategy, namely maximizing self-consumption (MSC) strategy. This case was used as a baseline.
- Case 2: The PV-battery-flexible load system operates under the optimal strategy, which was obtained via solving the developed many-objective optimal models.

3.2.1 Demand-side management of the PV-battery-flexible load system under the rule-based operation strategy

The operation of the PV-battery-flexible load system under the MSC strategy is illustrated in **Fig. 4**. The battery charges during the periods from 7:30 to 11:00, when the PV generation is sufficient, along with SOC increasing. When the SOC reaches the maximum, the battery stops charging with the surplus PV generation fed into the

utility grids. The electricity stored in the battery is released during the periods from 18:50 to 22:00, when the PV generation cannot meet household electricity loads. After all the stored electricity is discharged, households purchase electricity from the utility grid to satisfy the electricity demands. In addition to the battery, the flexible loads operate at normal conditions. AC1 operates with the temperature setpoint setting at 26 ^{o} C, while AC2 temperature setpoint sets at 25 ^{o} C. the EWH operates with the temperature setpoint keeping at 65 ^{o} C. The WM and the dishwasher are turned on at 6:30 and 19:00, respectively. Under the MSC operation strategy, the daily operation costs, peak-valley difference of net power profiles, SCR, SSR, and CO_2 emissions are 5.46 CNY, 5782.72 W, 53.06%, 63.17%, and 11.72 kg CO_2.

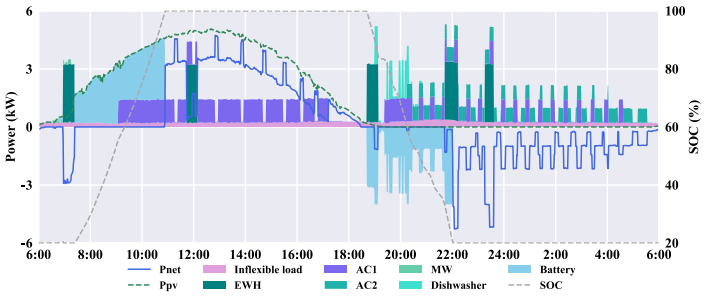

Fig. 4. *Operation of the PV-battery-flexible load system under the MSC strategy.*

3.2.2 Demand-side management of the PV-battery-flexible load system under the optimal strategy

The operation of the TCLs in the PV-battery-flexible load system under the optimal strategy is displayed in **Fig. 5**. It is observed that the temperature setpoints of TCLs are adjusted continuously to maximize the optimization objectives. However, the temperature setpoints always keep within the thermal comfort of occupants. Moreover, the WM and the dishwasher are switched on at 6:59 and 0:44, respectively. The operation of the PV-battery-flexible load system under the optimal strategy is presented in **Fig. 6**. The charging/discharging power of the battery is managed. It charges in the daytime, when the PV generation is sufficient, and the surplus PV generation is fed into the utility grids. The battery charges at night, when there is no PV generation. Almost all the peak loads during the high price periods can be met by the battery. The loads after 23:00 are satisfied by the utility grid, owing to the fact that the electricity stored in the battery is consumed. Under the optimal operation strategy, the daily operation costs, peak-valley difference of net power profiles, SCR, SSR, and CO_2 emissions are 3.36 CNY, 4771.04 W, 55.91%, 68.80%, and 9.61 kg CO_2. However, user's dissatisfaction is raised to 0.16 due to the adjustment of TCLs' temperature setpoints and the shifting of deferrable loads.

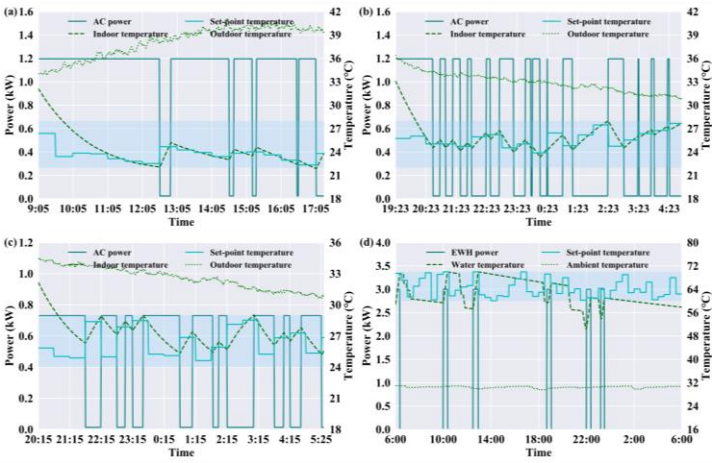

Fig. 5*. Operation of flexible loads in the PV-battery-flexible load system under the optimal strategy.*

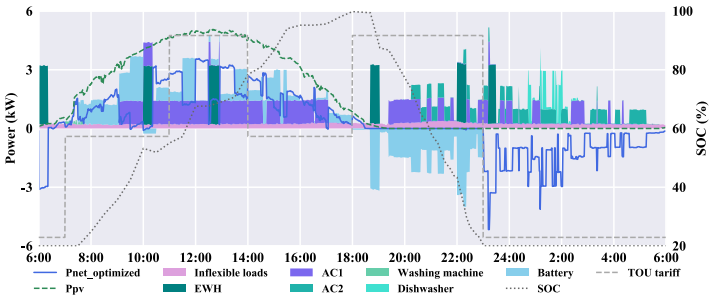

Fig. 6. *Operation of the PV-battery-flexible load system under the optimal strategy.*

3.2.3 Comparative analysis of the demand-side management of PV-battery-flexible load system under the rule-based strategy and the optimal strategy

A comparative analysis on the performance of the PV-battery-system was conducted under diverse operation strategies, as illustrated in **Fig. 7**. It is observed that the optimal operation strategy performs better in daily operation costs, peak-valley difference, SCR, SSR, and CO_2 emissions aspects than the MSC strategy. The daily operation costs, CO_2 emissions, and the peak-valley difference are decreased by 38.4%, 18%, and 17.5% under the optimal strategy, when compared with the MSC operation strategy. The reasons are that the electricity consumption of TCLs is decreased under the optimal strategy, thus the electricity imported from the utility grids is reduced, contributing to a reduction of CO_2 emissions. Moreover, since some peak loads are shifted

to valley-price periods, which can be found via comparing **Fig. 4** and **Fig. 6**, the electricity bills are decreased. Furthermore, the optimization of TCLs' temperature setpoint, deferrable loads' working time, and the charging/discharging power contributes to the peak cutting and valley filling. Hence, the peak-valley difference is smaller under the optimal strategy. Compared with the MSC strategy, the SCR and SSR under the optimal strategy are increased by 5.4% and 8.9%, respectively. More loads are shifted to the daytime when PV generation is sufficient under the optimal strategy. Therefore, the PV generation consumption is increased under the optimal strategy. However, user's dissatisfaction is raised to 0.16 under the optimal strategy, which is caused by the adjustment of TCLs temperature setpoint and the shifting of deferrable loads' working time.

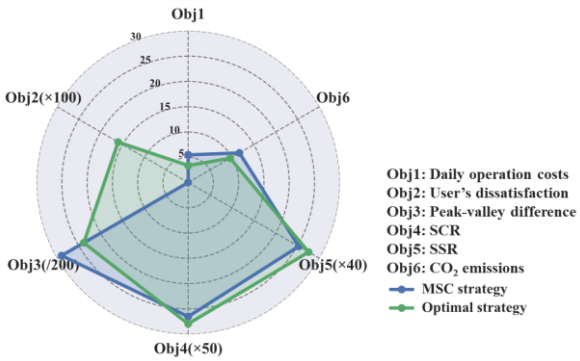

Fig. 7. *Comparison of the system performance under various operation strategies.*

4. CONCLUSIONS

A many-objective optimal model was developed for the day-ahead optimal scheduling of residential PV-battery-flexible load systems, with six optimization objectives relevant to the benefits of diverse stakeholders considered. A case study was conducted to validate the many-objective optimal model based on the monitored real-life operation data. Comparative studies about the operation of the system under the optimal strategy and the MSC strategy was also conducted. Results indicate that the daily operation costs, CO_2 emissions, and the peak-valley difference are decreased by 38.4%, 18%, and 17.5% under the optimal strategy with the SCR and SSR increasing by 5.4% and 8.9%, when compared with the MSC operation strategy. In our future work, the real-time optimal scheduling of residential PV-battery-flexible load system will be carried out.

ACKNOWLEDGEMENT

This work was financially supported by the National Key R&D Program of China (2022YFB4201003), the National Natural Science Foundation of China (52278104), and the Science and Technology Program of Ministry of Housing and Urban-Rural Development of the PRC (2020-K-165).

DECLARATION OF INTEREST STATEMENT

The authors declare that they have no known competing financial interests or personal relationships that could have appeared to influence the work reported in this paper. All authors read and approved the final manuscript.

REFERENCE

[1] Ouedraogo KE, Ekim PO, Demirok E. Feasibility of low-cost energy management system using embedded optimization for PV and battery storage assisted residential buildings. Energy 2023;271. https://doi.org/10.1016/j.energy.2023.126922.

[2] Chen Z, Chen Y, He R, Liu J, Gao M, Zhang L. Multi-objective residential load scheduling approach for demand response in smart grid. Sustain Cities Soc 2022;76. https://doi.org/10.1016/j.scs.2021.103530.

[3] Zou B, Peng J, Yin R, Luo Z, Song J, Ma T, et al. Energy management of the grid-connected residential photovoltaic-battery system using model predictive control coupled with dynamic programming. Energy Build 2023;279:112712. https://doi.org/10.1016/j.enbuild.2022.112712.

[4] Killian M, Zauner M, Kozek M. Comprehensive smart home energy management system using mixed-integer quadratic-programming. Appl Energy 2018;222:662–72. https://doi.org/10.1016/j.apenergy.2018.03.179.

[5] Yang F, Xia X. Techno-economic and environmental optimization of a household photovoltaic-battery hybrid power system within demand side management. Renew Energy 2017;108:132–43. https://doi.org/10.1016/j.renene.2017.02.054.

[6] Zhi Y, Yang X. Scenario-based multi-objective optimization strategy for rural PV-battery systems. Appl Energy 2023;345:121314. https://doi.org/10.1016/j.apenergy.2023.121314.

[7] Wang Z, Sun M, Gao C, Wang X, Chris B. A new interactive real-time pricing mechanism of demand response based on an evaluation model. Appl Energy 2021;295:117052. https://doi.org/https://doi.org/10.1016/j.apenergy.2021.117052.

[8] Wang M, Peng J, Luo Y, Shen Z, Yang H. Comparison of different simplistic prediction models for forecasting PV power output: Assessment with experimental measurements. Energy 2021;224. https://doi.org/10.1016/j.energy.2021.120162.
[9] Zou B, Peng J, Li S, Li Y, Yan J, Yang H. Comparative study of the dynamic programming-based and rule-based operation strategies for grid-connected PV-battery systems of office buildings. Appl Energy 2022;305. https://doi.org/10.1016/j.apenergy.2021.117875.
[10] Mulleriyawage UGK, Shen WX. Optimally sizing of battery energy storage capacity by operational optimization of residential PV-Battery systems: An Australian household case study. Renew Energy 2020;160:852–64. https://doi.org/10.1016/j.renene.2020.07.022.
[11] Jin X, Baker K, Christensen D, Isley S. Foresee: A user-centric home energy management system for energy efficiency and demand response. Appl Energy 2017;205:1583–95. https://doi.org/10.1016/j.apenergy.2017.08.166.
[12] Hu M, Xiao F. Investigation of the demand response potentials of residential air conditioners using grey-box room thermal model. Appl Energy 2017;207:324–35. https://doi.org/10.1016/j.apenergy.2017.05.099.
[13] Pascual J, Arcos-Aviles D, Ursúa A, Sanchis P, Marroyo L. Energy management for an electro-thermal renewable–based residential microgrid with energy balance forecasting and demand side management. Appl Energy 2021;295. https://doi.org/10.1016/j.apenergy.2021.117062.
[14] Deb K, Jain H. An evolutionary many-objective optimization algorithm using reference-point-based nondominated sorting approach, Part I: Solving problems with box constraints. IEEE Trans Evol Comput 2014;18:577–601. https://doi.org/10.1109/TEVC.2013.2281535.